

INITIAL OXIDE PARTICLE DEPOSITION UNDER LOW-TEMPERATURE COOLING WATER CONDITIONS: EXPERIMENTS UNDER SUBCOOLED BOILING AT HIGH pH

K. Khumsa-Ang¹ and D.H. Lister²

Department of Chemical Engineering, University of New Brunswick, PO Box 4400, Fredericton, NB, Canada, E3B 5A3
¹ kittima.k@unb.ca, ² dlister@unb.ca

ABSTRACT

The deposition behaviour of colloidal corrosion-product particles under isothermal conditions and different modes of heat transfer at atmospheric pressure has been reported previously – under conditions where the particles and heat-transfer surface had opposite electrostatic charges so the fouling process was under transport control. Reported here are observations from a recirculating loop of the deposition of nickel ferrite from suspension in alkaline water during sub-cooled boiling at the surface of an Alloy-800 tube. Control was nominally by attachment. The experiment involved tracing the particles with radioactive ⁶⁰Co so that their accumulation on the tube could be monitored remotely. A radioactive scoping test lasting 147h was followed by a test with three continuous, sequential periods when the surface radioactivity was monitored. The first, for 117 h, involved exposure to a ~5-ppm suspension, followed by a 124-h exposure to a nominally identical but non-radioactive suspension, followed by a 68-h exposure to water nominally devoid of nickel ferrite. The deposition during the first period followed kinetics similar to those measured under transport control in previous experiments and could be described by a mechanistic model developed previously. The surface radioactivity during the second period decreased, even whilst non-radioactive particles continued to deposit, but tended towards an asymptotic value at a rate that suggested that consolidation of a large portion of the deposit occurred abruptly. The final period saw a further decrease in surface radioactivity, presumably due to dissolution and release of deposit in the solute-free environment. These results are described with a mathematical model and their implications discussed in the context of the previous experiments.

INTRODUCTION

Fossil-fired and nuclear power plants are heat transfer systems devoted to converting thermal energy to electricity through a steam turbine cycle. They incorporate many heat exchangers besides the principal boiler/steam-generator or reactor. Typical exchangers along the feed-train from the condenser, for example, raise the feed-water temperature in stages to improve the thermal efficiency, and in a typical nuclear plant up to seven or so feed-water heaters raise the temperature from about 30°C to about 180°C. There are also many water-cooled exchangers operating at relatively low temperatures for systems other than the main steam

cycle. The fouling of these units can have serious implications for the operation of the plant, both in terms of the loss of efficiency and the potential for under-deposit corrosion. Since corrosion-product oxides are major contributors to the fouling of cooling-water exchangers, elucidating the mechanisms by which they deposit on heat transfer surfaces under a range of conditions has been the aim of our on-going research program. The focus has been the initial period of fouling, when the deposit characteristics are being established.

Oxides commonly found in cooling water systems are particulate ferrites such as magnetite. The mechanisms of fouling by particles have been postulated to consist of the interplay of several processes occurring in concert: particle transport from suspension in the bulk coolant; attachment to the deposit; concomitant removal from the deposit as deposition proceeds (by some exchange mechanism); and, consolidation of the deposit at the heat-transfer surface (Kern and Seaton, 1959; Gudmundsson, 1981; Epstein, 1988, Turner and Godin, 1994; Basset et al., 2000, Klimas and Pietralik, 2002). When boiling occurs, additional particle transport, removal and consolidation mechanisms are introduced (Charlesworth, 1970; Thomas and Grigull, 1974; Asakura et al., 1978).

The first two processes make up the deposition stage, involving the transport of particles from the main fluid stream to the heat transfer surface either by diffusion or inertia, followed by the attachment of those particles to the surface that may be already covered with deposit. Since the particles and surface develop surface charges depending upon their PZC (point of zero charge) and the pH of the coolant, the deposition may be transport-controlled (if the charges are of different sign and therefore attractive) or attachment-controlled (if the charges are of like sign and repellent). The deposit itself is subject to consolidation by a process of aging at the heat transfer surface, while removal occurs from the unconsolidated or labile portion. The onset of consolidation is an important factor in establishing the basis for a permanent deposit, since it is not conceivable that a heavy deposit can be completely labile and subject to concomitant removal/deposition. There must, however, be a labile portion that remains accessible to the coolant for as long as such removal continues – presumably in a layer above the consolidated portion in a well-established deposit. The deposit evolution is shown schematically in Figure 1.

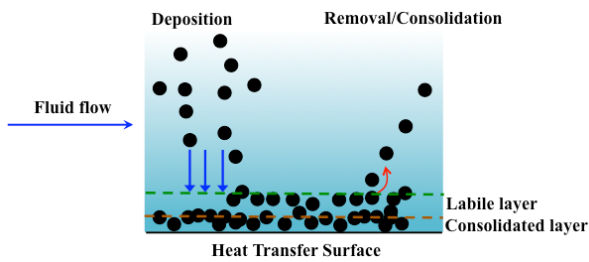


Figure 1: Schematic representation of particulate deposition.

The laboratory program at UNB investigates the first few hundred hours of deposition of particles of corrosion-product oxides from suspension in water at atmospheric pressure onto Alloy-800 surfaces under isothermal conditions and under different modes of heat transfer. The results of experiments on the deposition of colloidal magnetite and nickel ferrite under a range of heat transfer modes (isothermal, convective, subcooled boiling and bulk boiling) were reported earlier (Margotin, 1994; Callamand et al., 1999; Basset et al., 2000; Carpentier et al., 2001; Cossaboom and Lister, 2005).

In general, after particle transport from the bulk and adherence to the surface, deposit removal and consolidation have a greater effect on the overall deposition under boiling conditions than under non-boiling conditions. Thus, at neutral pH and under subcooled boiling, removal of magnetite particles was an active mechanism but the deposit had little tendency to consolidate (Basset et al., 2000). Also at neutral pH but under bulk boiling, nickel ferrite deposits displayed removal and also consolidated (Cossaboom and Lister, 2005). To describe the mechanisms behind these findings, a global equation to predict the deposition flux under transport-controlled conditions was proposed (Lister and Cussac, 2009). The model takes into account the size, nucleation frequency and nucleation-site geometry of bubbles based on microlayer evaporation theory (Asakura et al., 1978) as well as observations of particle behaviour in bubbling regimes. It was in good agreement with experimental results.

Recently, preliminary experiments on the deposition of nickel ferrite under subcooled boiling conditions at pH 9.5-10.0 (to impose nominal attachment control by making surfaces of both the particles and the Alloy-800 tube negatively charged) have been reported (Khumsa-Ang and Lister, 2009). Interestingly, the results agreed with the model predictions, even though the model was derived for transport control.

The work reported here extends those preliminary experiments and quantifies the kinetics of both deposition and removal of nickel ferrite particles under the same conditions. Using a radiotracing technique, concomitant release (when a continuous source of suspended particles is available in the coolant) and non-concomitant release (when the coolant is free of particles) are studied. The experimental results are used to modify the traditional particulate fouling model first formulated by Kern and Seaton (1959) by incorporating mechanistic terms, and the

model is validated with the results of the preliminary, non-radioactive experiments.

EXPERIMENTAL TECHNIQUES

The experiments involve the synthesis of nickel ferrite particles and the study of their deposition in a recirculating fouling loop under operating conditions similar to those of low-pressure, low-temperature heat exchangers. The loop, which has been described before (Khumsa-Ang and Lister, 2009), is made mostly of stainless steel but has a vertical glass column as test section, 1.5 m long and 10 cm diameter. The heat-exchange surface is provided by a tube of Alloy 800, 50 cm long and 1.6 cm diameter, mounted in the top of the column and containing a heating cartridge capable of generating a heat flux at the tube surface of 140 kW/m^2 . Water coolant is supplied to the bottom of the test section from three tanks by a pump delivering up to 12 L/min. At the temperature of the experiments, 90°C at the test section entrance, this gives a Reynolds number in the annulus around the heater tube of $\sim 10,000$. For the experiments reported here, subcooled boiling began about 3 cm from the beginning of the heater (from the “nose”) and by about 40 cm had intensified to bulk boiling. The loop has two 170-L tanks and one 20-L tank which are valved into the circuit individually; the first two are generally filled with suspensions of corrosion products while the last and smallest is filled with water conditioned to the same pH as the other two (see Figure 2).

The preliminary experiments (Khumsa-Ang and Lister, 2009) used nonstoichiometric nickel ferrite particles (called Type A) synthesized by a solid-state technique (Cossaboom and Lister, 2005). These later experiments used similar material except traced with cobalt in order to incorporate radioactivity. The three types are as follows:

Type A – nonradioactive nickel ferrite ($\text{Ni}_x\text{Fe}_{3-x}\text{O}_4$), $0.48 \leq x \leq 0.56$;

Type B – radioactive nickel ferrite traced with ^{59}Co activated with ^{60}Co (designated $^{60}\text{Co}_{0.14}\text{Ni}_{0.46}\text{Fe}_{2.4}\text{O}_4$);

Type C – nonradioactive nickel ferrite traced with ^{59}Co ($\text{Co}_{0.14}\text{Ni}_{0.46}\text{Fe}_{2.4}\text{O}_4$).

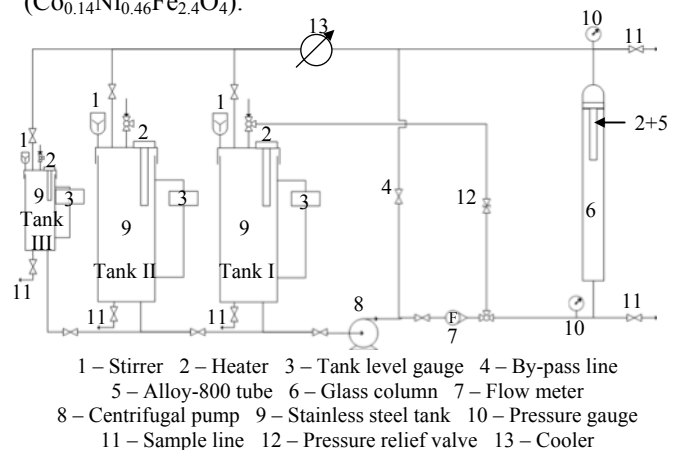


Figure 2: Schematic diagram of the fouling loop.

Cobalt-60 was used for radiotracing Type B material because of its strong gamma-ray emission (easily identifiable with gamma spectrometry at peak energies of 1.13 MeV and 1.27 MeV) and moderate half-life (5.2 years). After synthesis, the non-radioactive material was

characterised with scanning electron microscopy (SEM), energy-dispersive x-ray emission (EDX) and x-ray diffraction (XRD). The PZC was determined with a Zeta-meter. The results from the Type C material were assumed to apply to the radioactive Type B material. The synthesised particles had a fairly narrow size distribution in the colloidal range (0.5 μm to 0.8 μm) and were nearly spherical. Their PZC was measured at pH 4.7 and measurements of filings of Alloy 800 indicated that the heater tube would have a PZC of 4.4.

The off-line "counting" of radioactivity used a high-purity germanium gamma detector with a Canberra S100 multi-channel analyser. For each counting sequence the detector was cooled with liquid nitrogen and its head mounted in a standard position in a lead castle to minimise interference from background radiation. The counting geometry was calibrated using a ^{60}Co source of known intensity (38.85 kBq as received on June 5, 2009). On-line counting of radioactivity deposited on the heater tube used the detector mounted in front of the glass column at a height corresponding to part-way up the tube. The detector head was enclosed in a lead shield with a collimating slit (7 mm by 25 mm) in the front wall that allowed a portion of the tube to be monitored. The on-line system was calibrated after an experiment by removing a portion of the deposit from a given area of the tube that had been in front of the detector and counting it off-line in the calibrated geometry. During radioactive experiments, the activity of ^{60}Co recorded from the detector was logged on-line every hour.

Type B (radioactive) nickel ferrite particles were in suspension in Tank I at a concentration of 5 part per million (ppm), Tank II contained a (nonradioactive) suspension of Type C particles at the same concentration and Tank III contained only water. All tanks were adjusted to pH 10 with KOH and Tank I was shielded with concrete blocks and lead bricks to minimize background radiation.

An experiment with radioactivity began with the circulation of loop water at temperature (90°C) through the loop and Tank I for at least 24 h prior to the installation of the heater tube; this established an initial background counting rate for the detector in front of the test section. The heater tube was then installed in the top of the test section and connected to the power supply so that bulk boiling began about 80% of the way along its length. For the first run, Run 2.1, the build-up of radioactivity was monitored for 147 h, the heater tube removed, and counting continued for a further 42 h to establish the final background count rate. The second run, Run 2.2, proceeded similarly, except that radioactivity build-up on the heater was monitored for 117 h with only Tank I valved in, then only Tank II was valved in for 124 h to monitor the evolution of radioactivity as non-radioactive particles continued to deposit, then only Tank III was valved in (for 68 h) to see how the radioactivity reacted to water free from particles. For both runs, the data were corrected for radioactive decay to the start of the experiment (although the correction was small), and were reduced by values of background interpolated linearly from the measurements before and after the run. Samples of coolant were removed every twelve hours from

the line at the top of the test section for off-line counting and chemistry analysis.

After the heater was removed at the end of a run, the deposit on a 2-cm² area of the monitored section that had been in front of the detector was removed by polishing and swabbing with HCl solution; the resulting solution was analysed for dissolved iron and ^{60}Co activity to indicate the surface concentration of deposit and its activity. Table 1 summarises the conditions of this study and of the preliminary experiments.

Table 1: Loop operating conditions for nickel ferrite deposition: $\text{Re} = 10,000$, heat flux = 112 kW/m², temperature = 90°C, $\text{pH}_{25^\circ\text{C}} = 10$.

Run no.	Type of suspension	Exposure time (h)
1.1*	Nonradioactive nickel ferrite (Type A)	170 h deposition 22 h non-concomitant removal
1.2*	Nonradioactive nickel ferrite (Type A)	170 h deposition 22 h non-concomitant removal
2.1	Radioactive nickel ferrite traced with ^{60}Co (Type B)	147 h deposition
2.2	Radioactive nickel ferrite traced with ^{60}Co (Type B), non-radioactive nickel ferrite traced with ^{59}Co (Type C), particle-free coolant	117 h deposition 124 h concomitant removal 68 h non-concomitant removal

* preliminary experiments conducted previously (Khumsang and Lister, 2009).

EXPERIMENTAL RESULTS

Figure 3 presents the build-up of radioactivity and the corresponding build-up of mass of nickel ferrite on the Alloy-800 tube for the first 110 h of Runs 2.1 and 2.2.

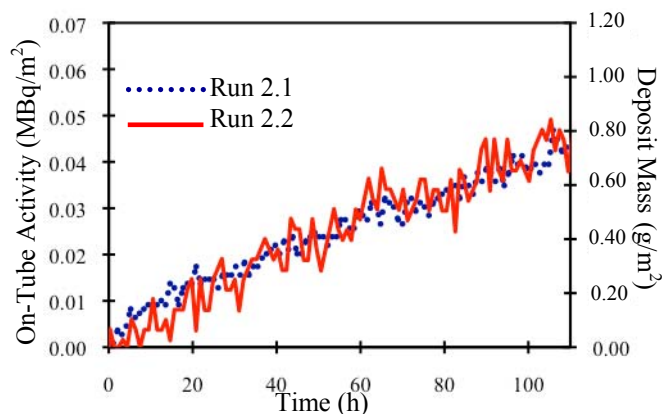


Figure 3: Nickel ferrite deposition on Alloy-800 tube in terms of activity and converted mass for the first 110 hours of Runs 2.1 and 2.2.

The agreement between the runs is good, although the data were more scattered in Run 2.2 – no doubt due to the

difficulty in maintaining a constant source term (there was poor mixing in the coolant tank during this run) and increased counting error from a higher background.

In Run 2.2, the source was switched from the suspension of active nickel ferrite (Type B in Tank I) to the suspension of non-radioactive nickel ferrite (Type C in Tank II) after 117 hours. The on-tube radioactivity decreased, even though particles continued to deposit. After a further 124 hours, the coolant source was switched to particle-free water in Tank III and more release of radioactivity occurred. The evolution of radioactivity is shown in Figure 4. Note that the initial rapid decrease in radioactivity in the final period indicates that a different release mechanism was in operation.

During the deposition period in Runs 2.1 and 2.2, when Tank I was valved in, the specific activity of the deposit and the suspended particles was constant; the conversion of deposited radioactivity to units of mass of nickel ferrite was therefore straightforward (see Figure 3). In Run 2.2, however, switching between Tanks I and II steadily diluted the deposited activity so that there was no straightforward conversion of measured radioactivity to mass. Results in Figure 4 are therefore presented solely in term of surface radioactivity (MBq/m^2).

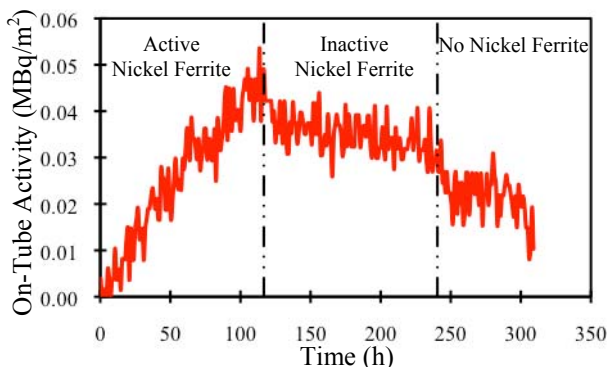


Figure 4: Radioactive nickel ferrite deposition on Alloy-800 tube in Run 2.2.

A decrease in the activity on the tube surface after the switch to the inactive nickel ferrite proves that particle removal concomitant with deposition is an active mechanism; if such removal had been negligible, the on-tube activity would have remained constant after the tank switch. Note also that the mass of deposited nickel ferrite would have continued building up with a pattern following the extrapolation of the activity deposition in the first 117 hours in Figure 4.

The evolution of the source term (activity of nickel ferrite per unit volume in suspension) was also monitored during Run 2.2 as shown in Figure 5. The activity of samples was very variable during the first 117 hours since active nickel ferrite was periodically added to the tank to maintain the target bulk concentration (poor mixing in the tank in this run allowed material to settle, and intermittent hide-out and release of particles within the loop and the sample line were suspected). To ensure that the source term was in fact the particles, two sets of ten 50 mL coolant samples were withdrawn from the sample line downstream of the test section just after an addition to Tank I. The first

set was filtered with 0.2- μm filter paper and then all samples were counted off-line for ^{60}Co radioactivity. As shown in Figure 6, the activity of the particles in the unfiltered samples was dominant, although there was a small value above the average background indicated for the filtered samples (about 3% of the unfiltered value). This suggests that a small amount of dissolution may have occurred; it may have contributed to the removal processes when the coolant from Tank III was circulating through the test section.

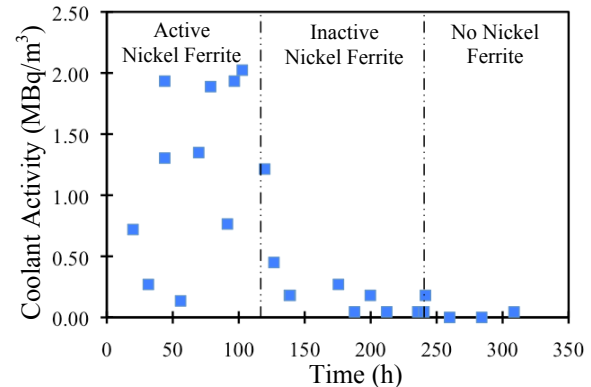


Figure 5: Evolution of nickel ferrite activity in coolant in Run 2.2.

After the switches to the inactive and then particle-free tanks, the coolant activity decreased significantly and eventually reached zero at the end of the experiment. During the first release period, the rate of decrease of deposited activity on the heater tube diminished and the deposited amount tended to level off at a finite value, suggesting that the deposit was consolidating. The trend in the final release period is not so clear, although continuing release below the previous consolidated level is indicated.

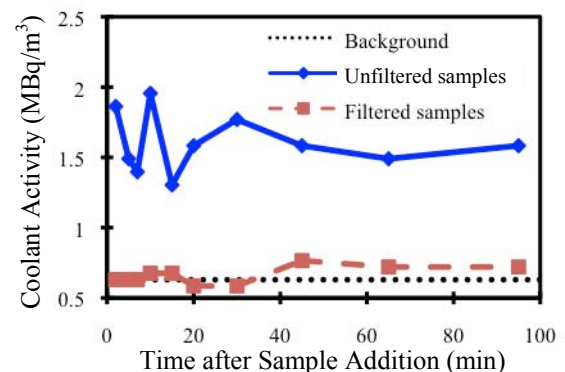


Figure 6: Activities of filtered and unfiltered coolant after an addition of radioactive nickel ferrite particles to Tank I in Run 2.2.

In the preliminary experiments Runs 1.1 and 1.2 reported earlier (Khumsa-Ang and Lister, 2009), the amount of deposit was measured after 170 h and the release of deposited mass to particle-free coolant was measured at intervals during a further 22 h. Those release measurements are compared with results from the final release period of Run 2.2 in the normalised Figure 7. The behaviour in all three runs was similar; the initial removal rate was rapid and diminished with time, and in Run 2.2 and the longer release

experiment of Run 1.2 the deposit reached about 30% of the initial value in about 70 h.

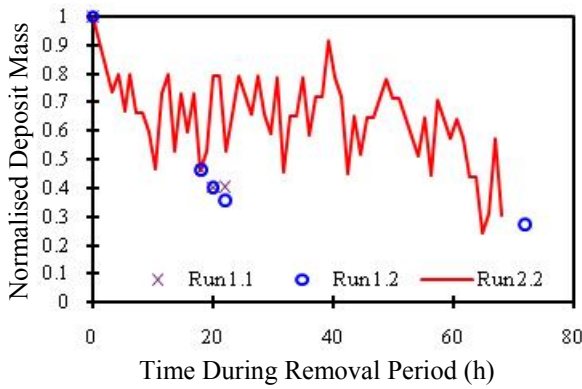


Figure 7: Normalised deposit removal measurements in particle-free coolant: non-radioactive experiments (Runs 1.1 and 1.2) and radioactive experiment (Run 2.2).

DISCUSSION

Descriptions of particle deposition and release have previously been made in terms of empirical deposition and release coefficients (K_d and k_r respectively). Thus, after the approach of Kern and Seaton (1959):

Rate of change of deposit = Deposition rate – Removal rate

$$\frac{dm(t)}{dt} = K_d C_b - k_r m(t) \quad (1)$$

where C_b is the mass concentration of the source in the coolant. For an initial condition of zero deposit at time zero, the expression integrates to:

$$m(t) = \frac{K_d C_b}{k_r} (1 - \exp(-k_r t)) \quad (2)$$

It is usually assumed in the Kern-Seaton approach that the build-up in terms of deposited activity (A_T) is the same as that in terms of mass (Basset et al., 2000). Thus, we can rewrite Equation (2) (with the coolant Activity A_s), as:

$$A_T = \frac{K_d A_s}{k_r} (1 - \exp(-k_r t)) \quad (3)$$

At short times, Equations (2) or (3) will generally fit empirical data. At long times, however, the fact that the equations predict a build-up of deposit to an asymptotic value and are based on a release parameter that operates on the whole deposit often contradicts experimental results (e.g., Cossaboom and Lister, 2005). Modelling has attempted to overcome these deficiencies by introducing mechanistic details such as the consolidation of the deposit so that only a portion is available for release or exchange with the source term in the coolant (Turner and Klimas, 2001; Cossaboom and Lister, 2005; Lister and Cussac, 2009).

It is clear from the deposition data in Run 2.2 that the straightforward Kern-Seaton approach is inadequate here also (Figure 4). During the deposition of inactive particles after the first tank switch, concomitant release is levelling off and leaving a finite activity, rather than allowing complete removal of the activity. We account for this by postulating that the deposit is made up two portions – a

consolidated and a labile layer, of which only the latter is available for concomitant release. The mechanistic model of Lister and Cussac (2009) describes the formation of the layers in terms of the heat transfer parameters of the system, such as the heat flux, the intensity of boiling and the characteristics of the bubble nucleation sites.

FORMATION OF LABILE AND CONSOLIDATED LAYERS IN RUN 2.2

We introduce three terms to describe deposited nickel ferrite radioactivity: the labile, consolidated and total layers – respectively A_L , A_C and A_T , where A_T equals $A_L + A_C$ at any given time (t) as shown schematically in Figure 8 for the period before the first tank switch. The deposit only begins to consolidate at time t_c . During this period, the equivalent total mass, $m(t)$, behaves in the same manner as A_T .

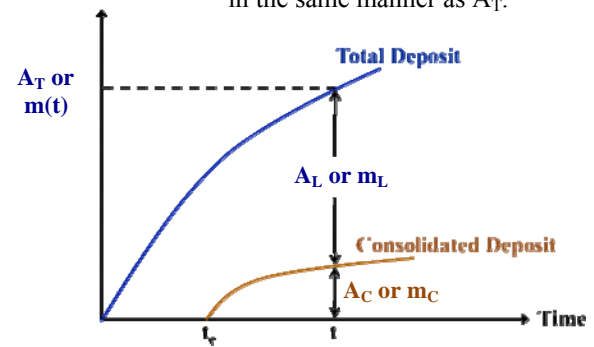


Figure 8: Schematic diagram of build-up of surface activity/mass in terms of labile and consolidated layers with constant source term (i.e., before first tank switch).

During the deposition period before the critical time t_c ($0 < t < t_c$), when the consolidation term is zero and the specific activity of the suspension is constant and equal to that of the labile layer (s_L), the deposition is described via Equations (1)-(3).

After the critical time, t_c , and before the first tank switch at t_1 ($t_c < t < t_1$), the consolidation term is introduced. It was previously defined (Turner and Klimas, 2001; Cossaboom and Lister, 2005; Lister and Cussac, 2009) as the fraction of deposit that is strongly bonded to the surface and is hard to remove. We found by trial and error that an empirical expression for the evolution of the consolidated layer, m_C , fitted the data from Run 2.2 best. The results of Cossaboom and Lister (2005) showed a leveling-off of the deposit during a release period, also suggesting that consolidation follows an asymptotic expression. Accordingly:

$$m_C = a_c \cdot (1 - \exp(-b_c (t - t_c))) \quad (4)$$

where m_C is the mass of consolidated particles (kg/m^2), t_c is the critical time when consolidation first occurs and a_c and b_c are consolidation constants with values 0.4 kg/m^2 and $5.5 \times 10^{-6} \text{ s}^{-1}$. Previous studies (Turner and Klimas, 2001; Lister and Cussac, 2009) assumed different functions in order to describe the data, but under different experimental conditions.

Noting that for times below t_c the whole deposit is labile and $m(t)$ and A_T can be calculated by Equations (2) and (3). In general, after the consolidated layer is formed ($t > t_c$), we can write:

Rate of change of mass of labile layer = Mass deposition rate – Rate of removal of labile mass – Rate of change of mass of consolidated layer

$$\frac{dm_L}{dt} = K_d C_b - k_r m_L - \frac{dm_C}{dt} \quad (5)$$

where m_L is the amount of labile deposit (kg/m^2), which is readily exchanged with the particles in the coolant. The initial conditions are: at $t = t_c$, $m_L = m(t_c)$. In terms of activity and assuming homogeneity of the layers:

Rate of change of activity of the labile layer = Activity deposition rate – Rate of removal of surface activity – Rate of change of activity of consolidated layer

$$\frac{dA_L}{dt} = K_d A_s - k_r A_L - \frac{dA_C}{dt} \quad (6)$$

The initial conditions are: at $t = t_c$, $A_L = A_L(t_c)$ and $A_L(t_c) = s_{L1} \cdot m(t_c)$, where $m(t_c)$ is the mass of deposit at the critical time and s_{L1} is the specific activity of the labile layer, which equals the specific activity of the suspended particles in the first period ($t < t_1$). Here it will be $dA_C/dt = dm_C/dt \cdot s_{L1}$ since $A_C/m_C = A_L/m_L = s_{L1}$. Equation (6) can be obtained by multiplying Equation (5) with s_{L1} .

Equations (5) and (6) are solved individually and by multiplying m_L by s_{L1} , A_L is expressed by Equation (8):

$$m_L = m(t_c) \cdot \exp(-k_r(t - t_c)) + \frac{K_d C_b}{k_r} (1 - \exp(-k_r(t - t_c))) + \left(\frac{a_c b_c \exp(-b_c(t - t_c))}{b_c - k_r} \right) (1 - \exp((b_c - k_r)(t - t_c))) \quad (7)$$

$$A_L = A_L(t_c) \cdot \exp(-k_r(t - t_c)) + \frac{K_d A_s}{k_r} (1 - \exp(-k_r(t - t_c))) + \left(\frac{s_{L1} a_c b_c \exp(-b_c(t - t_c))}{b_c - k_r} \right) (1 - \exp((b_c - k_r)(t - t_c))) \quad (8)$$

where $m(t) = m_L + m_C$ and $A_T = A_L + A_C$ at any given time.

During the second period ($t_1 < t < t_2$), after the tank is switched to that containing non-radioactive particles and concomitant “release” of activity from the surface is observed, the specific activity of the labile layer decreases from s_{L1} , since it is diluted by the deposition of inactive particles. The rate of change of mass of the labile layer, however, remains unaffected and is given by Equation (5) with initial conditions: at $t = t_1$, $m_L = m_L(t_1)$, $A_C = A_C(t_1)$ and $A_L = A_L(t_1)$. In terms of activity:

Rate of change of activity of the labile layer = – Rate of removal of surface activity – Rate of change in consolidated layer

$$\frac{dA_L}{dt} = -k_r A_L - \frac{dA_C}{dt} \quad (9)$$

and the change in the activity consolidation is described as:

$$\frac{dA_C}{dt} = \frac{dm_C}{dt} \cdot s_L(t) \text{ where } s_L(t) = \frac{A_L(t)}{m_L(t)} \quad (10)$$

leading to:

$$\frac{dA_C}{dt} = \frac{dm_C}{dt} \cdot \frac{A_L}{m_L} \quad (11)$$

and:

$$\frac{dA_L}{dt} = -k_r A_L - \frac{dm_C}{dt} \cdot \frac{A_L}{m_L} \quad (12)$$

The initial conditions are: at $t = t_1$, $m_L = m_L(t_1)$, $A_C = A_C(t_1)$, $A_L = A_L(t_1)$; Equations (5), (11) and (12) were solved simultaneously using Linear ODE Function in computer code Polymath. The resulting evolution of surface activity of nickel ferrite between t_1 and t_2 is shown in Figure 9.

During the non-concomitant removal period ($t_2 < t < t_3$), only Tank III containing particle-free coolant was valved into the circuit and the specific activity of the labile layer was therefore constant at s_{L2} (i.e., $s_L(t_2)$). There is no further deposition in this period and the surface activity continues to decrease (see Figure 9) but at a higher rate, suggesting that another removal mechanism works cooperatively with the particle removal mechanism proposed for the labile layer. It is postulated that the mechanism is dissolution, since the particle-free coolant in Tank III will also be solute-free (at least initially) and will tend to dissolve all parts of the deposit as well as continue to remove particles from the labile layer.

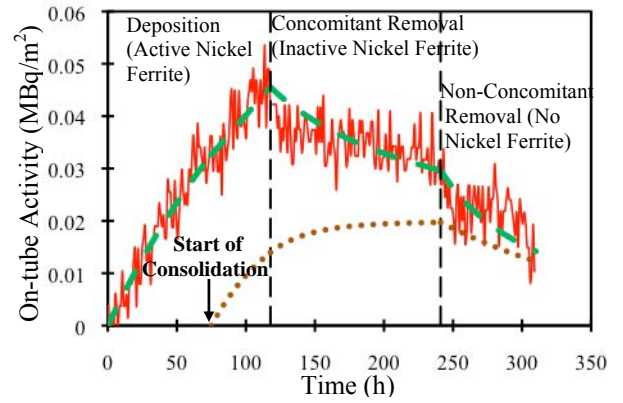


Figure 9: Nickel ferrite (activity) deposition on Alloy-800 tube in Run 2.2 with model fit: — experimental data, — — total activity prediction and consolidated layer prediction.

Since both the labile and consolidated layers dissolve, m_C (for the consolidated layer) is defined for period 3 with the effect of dissolution:

$$\frac{dm_C}{dt} = a_c b_c \exp(-b_c(t - t_c)) - k_{diss} m_C \quad (13)$$

The term m_L is defined for the labile layer where dm_C/dt is the first term on the RHS of Equation (13), which describes the continuing consolidation:

$$\frac{dm_L}{dt} = -k_r m_L - \frac{dm_C}{dt} - k_{diss} m_L \quad (14)$$

The initial conditions are: at $t = t_2$, $m_L = m_L(t_2)$ and k_{diss} is the dissolution rate constant of nickel ferrite particles.

For the activity of the labile layer in period 3:

$$\frac{dA_L}{dt} = -k_r A_L - \frac{dm_C}{dt} \cdot s_{L2} - k_{diss} A_L \quad (15)$$

where s_{L2} is the specific activity of the labile layer at $t = t_2$. Also in period 3, $A_C/m_C = A_L/m_L = s_{L2}$ and initial conditions

are: at $t = t_2$, $m_C = m_C(t_2)$, $m_L = m_L(t_2)$ and $A_L = A_L(t_2)$, leading to expressions for A_C as well as A_L and, thus, A_T .

Equations (14) and (15) are solved with Polymath. The results are shown in Figures 9 and 10, which also show the variations with time of deposited activity and of deposited mass of nickel ferrite, respectively, for the whole experiment.

An implication from Figure 10 is that the consolidated layer has almost levelled off by the time of the second tank switch, while the labile layer continues to thicken. This is a consequence of the mathematical function chosen for the consolidation (Equation (4)) to represent best the rather scattered data; it is not expected to be universally applicable, although similar behavior was observed before (Cossaboom and Lister, 2005). We can speculate that the mechanism is the growth of particles next to the surface by a crystallization mechanism that is affected by local increases in temperature. This is consistent with the high-temperature results of Turner et al. (1993), who showed that steam-generator deposits contained more tenacious layers next to the heating surface.

Figure 10 indicates that at the start of period 3 at 241 h, the particle-free coolant contacting the test section had a drastic effect on the deposit. The mass of the labile layer is predicted to diminish rapidly and the deposit may be tending to level off at a low value some time after the labile layer has disappeared, since continuing dissolution will increase the dissolved Fe and Ni in the coolant and reduce the driving force for further dissolution.

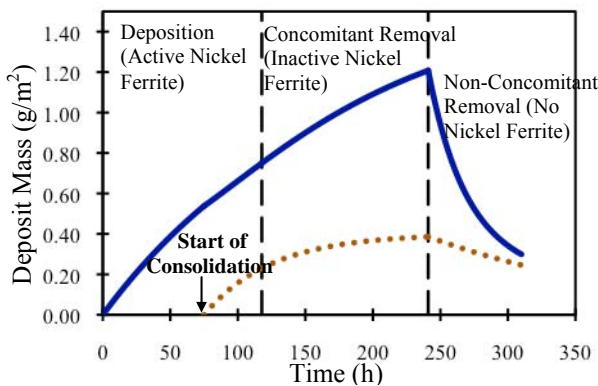


Figure 10: Model prediction of nickel ferrite (mass) deposition on Alloy-800 tube in Run 2.2 where — total deposit mass andconsolidated mass.

Tremaine and Leblanc (1980) reported the solubility of magnetite at pH 10 and 100°C to be 4.25×10^{-7} gFe/kg. Run 2.2 operated under similar temperature and chemistry conditions, and the filtration data in Figure 6 indicate approximately a solubility of the nickel ferrite particles of 2.8×10^{-4} gFe/kg. The dissolution rate of magnetite was reported by Balakrishnan (1977) to be 7.1×10^{-14} gFe/cm².s under somewhat similar conditions (pH 10.2 and 150°C). Our dissolution rate of nickel ferrite from the radioactive experiment Run 2.2 (from k_{diss} of 2.2×10^{-5} s⁻¹) is 4.45×10^{-12} gFe/cm².s. Our values are higher than those in the literature, perhaps indicating that the dissolution loosens the

deposit and promotes spalling but no doubt also reflecting the different oxides and experimental conditions.

According to the model fits in Figure 9, the predictions agree reasonably well with the experimental data and suggest that the premises of the mechanisms are sound. Table 2 shows a summary of the parameters for the model prediction in the radioactive experiment (Run 2.2).

Table 2: Summary of fitted parameters from the model prediction in Run 2.2.

Parameters and values	
Critical time to consolidation, t_c (h)	75
Deposition coefficient, K_d ($\mu\text{m/s}$)	0.14
Release coefficient, k_r (s ⁻¹)	1.8×10^{-6}
Consolidation constant, a_c (kg/m ²)	0.4
Consolidation constant, b_c (s ⁻¹)	5.5×10^{-6}
Dissolution coefficient, k_{diss} (s ⁻¹)	2.2×10^{-5}

Using the values from Table 2, the model was applied to the results of the preliminary, non-radioactive experiments (Runs 1.1 and 1.2). The comparisons between the predictions and the results are presented in Figure 11.

The model predicts reasonably well the non-radioactive experimental data. The differences between the measurements in both runs and the model predictions are between 10% and 27%, probably because measurements were made at different locations on the heater tube in the preliminary experiments and in Run 2.2. In other words-

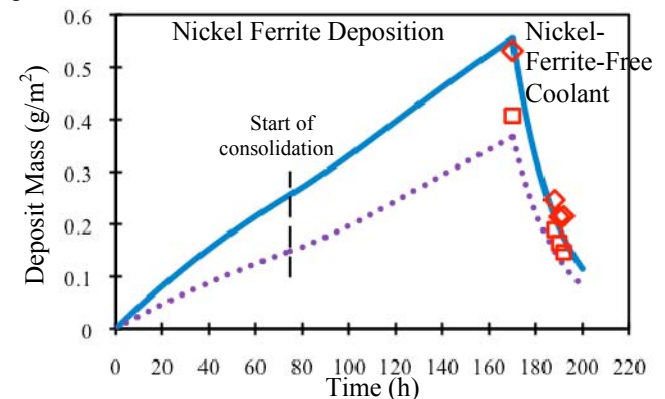


Figure 11: Predictions of nickel ferrite deposition for preliminary experiments Runs 1.1 and 1.2 where \diamond results from Run 1.1, \square results from Run 1.2, — Run 1.1 model fit, Run 1.2 model fit.

the mathematical model was derived from the radioactive experiment Run 2.2 in which the detector head measured the deposition occurring at the upper section on the heater (~35 cm from the heater nose), whereas the measurements from Runs 1.1 and 1.2 were averages made from areas of 1 cm by 2 cm at the middle and top sections on the heater at

19 cm and 40 cm from the heater nose, respectively. The boiling intensity increases, resulting in a higher removal rate, from the heater nose to the top as reported in the preliminary experiments (Khumsa-Ang and Lister, 2009). This results in a slightly lower estimate by the model.

Table 3 presents a summary of the results of fouling experiments and modelling over the last ten years or so in which radiotracing techniques were used under different operating conditions.

Table 3: Summary of parameter fits to radioactive experiments in the fouling loop.

	Khumsa-Ang and Lister (this study)	Lister and Cussac (2009)	Basset et al. (2000)	Cossboom and Lister (2005)
Iron oxide	Nickel ferrite	Magnetite	Magnetite	Nickel ferrite
Boiling mode	Subcooled	Subcooled	Subcooled	Bulk
q (kw/m²)	112	112	190	240
pH (nominal control)	9.5 (attachment)	7 (transport)	7 (transport)	7 (transport)
k_r (s⁻¹)	1.8×10 ⁻⁶	2.6×10 ⁻⁶	3.7×10 ⁻⁶	5.0×10 ⁻⁵
K_d (µm/s)	0.14	0.15	0.38	0.21
t_c (h)	75	51	-	-
b_c (s⁻¹)	5.5×10 ⁻⁶	3.3×10 ⁻⁶	-	6.9×10 ⁻⁶
k_{diss} (s⁻¹)	2.2×10 ⁻⁵	-	-	-

The fitted parameters are consistent, which is remarkable given the apparent variability of the source term in the current experiments. Surprisingly, there is little difference between the behaviour of magnetite and of nickel ferrite, nor between the effects of attachment control and transport control. The largest effect is due to heat flux, which includes a component due to the mode of boiling. The heat flux effect is expected; for example other, non-radiotraced, experiments in boiling had found an effect of the square of the heat flux on deposition rate (McCrea, 2001), in accordance with earlier results under more severe boiling conditions (e.g., Charlesworth, 1970).

CONCLUSIONS

1. First-order deposition/release kinetics cannot adequately describe fouling by corrosion-product particles during boiling under low-temperature cooling water conditions. Deposition, removal and consolidation (aging) may occur concomitantly and all must be taken into account.
2. A mathematical model has been formulated to describe deposition, removal and consolidation during the first

three hundred hours or so of the fouling process. To apply it to radiotracing experiments, the dilution of the specific activity of the labile layer during the concomitant particle deposition/removal period is taken into account. Model predictions are consistent with the results of non-radiotraced and radiotraced experiments.

3. The consolidated layer should form the foundation of a permanent deposit; determining its formation and properties will be important for predicting the long-term fouling of cooling-water heat exchangers.
4. In particle-free coolant, dissolution increases the removal rate of the labile layer significantly and also removes the consolidated layer.
5. For fouling by particulate corrosion products under low-temperature cooling water conditions, there is little effect of the nominal controlling process (attachment or transport) or of the type of oxide (magnetite or nickel ferrite). Heat flux has the greatest effect.

ACKNOWLEDGEMENTS

The authors acknowledge the Natural Sciences and Engineering Research Council of Canada and the CANDU® Owners Group for financial support and thank Keith Rollins, Adon Briggs and Piti Srisukvatananan for their assistance in the laboratory.

NOMENCLATURE

- a_c Consolidation constant (kg/m²)
- A_s Radioactivity of the coolant (MBq/m³)
- A_C Radioactivity of the consolidated layer (MBq/m²)
- A_L Radioactivity of the labile layer (MBq/m²)
- A_T On-tube radioactivity (MBq/m²)
- b_c Consolidation constant (1/s)
- C_b Concentration of the suspension (kg/m³)
- k_{diss} Dissolution rate constant (1/s)
- k_r Removal rate constant (1/s)
- K_d Deposition rate constant (m/s)
- m(t) Fouling mass at time t (kg/m²)
- m_C Mass of consolidated layer (kg/m²)
- m_L Mass of labile layer (kg/m²)
- q Heat flux (kW/m²)
- s_L Specific activity of the labile layer (MBq/g)
- t_c Critical time at the start of the consolidation (h)

REFERENCES

- Asakura, Y., Kikuchi, M., and Uchida, S., 1978, "Deposition of Iron Oxide on Heated Surfaces in Boiling Water", Nuclear Science and Engineering, Vol. 67 (1), pp. 1-7.
- Balakrishnan, P. V., 1977, "A Radiochemical Technique for the Study of Dissolution of Corrosion Products in

- High-Temperature Water”, *Canadian Journal of Chemical Engineering*, Vol. 55, pp. 357-360.
- Basset, M., McInerney, J., Arbeau, N., and Lister, D. H., 2000, “The Fouling of Alloy-800 Heat Exchange Surfaces by Magnetite Particles”, *Canadian Journal of Chemical Engineering*, Vol. 78, pp. 40-52.
- Callamand, S., Basset, M. and Lister, D. H., 1999, “Numerical Simulation of Corrosion Product Deposition on Heat Exchanger Surfaces”, *Proceedings of the International Conference on Mitigation of Heat Exchanger Fouling and Environmental Implications*, Banff, Canada, ECI Symposium Series, pp. 377-384.
- Carpentier, H., McCrea, L. and Lister, D. H., 2001, “Deposition of Corrosion Product Particles onto Heat Exchange Surfaces in Bulk Boiling”, *Proceedings of the Engineering Foundation International Conference on Heat Exchanger Fouling*, Davos, Switzerland, pp. 297-304.
- Charlesworth, D. H., 1970, “The Deposition of Corrosion Products in Boiling Water Systems”, *Chemical Engineering Progress Symposium Series*, Vol. 66 (104), pp. 21-30.
- Cossaboom, J. L., and Lister, D. H., 2005, “The Fouling of Alloy-800 Heat Exchanger Tubes by Nickel Ferrite Under Bulk Boiling Conditions”, *Proceedings of the 6th International Conference on Heat Exchanger Fouling and Cleaning*, Kloster Irsee, Germany, ECI Symposium Series RP2, pp. 109-118.
- Epstein, N., 1988, “Particulate Fouling of Heat Transfer Surfaces: Mechanisms and Models”, L. F. Melo Editor, *Fouling Science and Technology*, pp. 143-164.
- Gudmundsson, J. S., 1981, “Particulate Fouling” in: E. F. Somerscales and J. G. Knudsen, *Fouling of Heat Transfer Equipment*, Hemisphere Publishing Corporation, pp. 357-387.
- Kern, D. Q., and Seaton, R. E., 1959, “A Theoretical Analysis of Thermal Surface Fouling”, *British Chemical Engineering*, Vol. 4, pp. 258-262.
- Khumsa-Ang, K., and Lister, D. H., 2009, “The Investigation of Particulate Corrosion Product Deposition on Heat Transfer Surfaces: A Comparison of Experiments and Theory and a Preliminary Study of the Removal Mechanism”, *Proceedings of the 8th International Conference on Heat Exchanger Fouling and Cleaning*, Schladming, Austria, ECI Symposium Series, pp. 94-102.
- Klimas, S. J., and Pietralik, J. M., 2002, “Two-Phase Forced-Convective Fouling Under Steam Generator Operating Conditions”, *Proceedings of the 4th CNS International Steam Generator Conference*. Toronto, Canada.
- Lister, D. H., and Cussac, F., 2009, “Modelling of Particulate Fouling of Heat Exchanger Surfaces: Influence of Bubbles on Iron Oxide Deposition”, *Heat Transfer Engineering*, Vol. 30, pp. 840-850.
- Margotin, J-P., 1994, “Simulation of Corrosion Product Transport in Flowing Water” M.Sc. Thesis, Chemical Engineering, University of New Brunswick.
- McCrea, L., 2001, “Deposition of Corrosion Product Particles onto Heat Exchange Surfaces”, M.Sc. Thesis, Chemical Engineering, University of New Brunswick.
- Thomas, D., and Grigull, U., 1974, “Experimental Investigation of the Deposition of Suspended Magnetite from the Fluid Flow in Steam Generating Boiler Tubes”, *Proceedings, Brennst. Warme Kraft (Germany)*, Vol. 26, pp. 109-115.
- Tremaine, P. R., and Leblanc, J. C., 1980, “The Solubility of Magnetite and the Hydrolysis and Oxidation of Fe²⁺ in Water at 300°C”, *Journal of Solution Chemistry*, Vol. 9 (6), pp. 415.
- Turner, C. W., and Godin, M., 1994, “Mechanisms of Magnetite Deposition in Pressurized Boiling Water and Non-Boiling Water”, *Proceedings of the International Steam Generator and Heat Exchanger Conference*, Vol. 2, Toronto, Canada.
- Turner, C. W., Klimas, S. J., and Frattini, P. L., 1998, “Reducing Tube Bundle Deposition with Alternative Amines”, *Proceedings of the International Steam Generator and Heat Exchanger Conference*, Toronto, Canada.
- Turner, C. W., Lister, D. H., and Smith, D. W., 1990, “The Deposition and Removal of Sub-micron Particles of Magnetite at the Surface of Alloy-800”, *Proceedings of the International Steam Generator and Heat Exchanger Conference*, Toronto, Canada.
- Turner, C. W., Shamsuzzaman, K., and Tapping, R. L., 1993, “Factors Affecting the Consolidation of Steam Generator Sludge”, *National Association Corrosion Engineers (NACE 93)*, New Orleans, Louisiana.